Charge transfer in hyperthermal energy collisions of Li^+ with alkali-metal-covered Cu(001). II. Dynamics of excited-state formation

E. R. Behringer,* D. R. Andersson,† and B. H. Cooper
Laboratory of Atomic and Solid State Physics, Cornell University, Ithaca, New York 14853-2501

J. B. Marston
Department of Physics, Box 1843, Brown University, Providence, Rhode Island 02912
(Received 25 April 1996; revised manuscript received 24 July 1996)

We have measured the relative probability of excited state $[Li^0(2p)]$ formation versus the work-function change induced by alkali-metal adsorbates when hyperthermal energy Li^+ ions are incident on alkali-metal-covered Cu(001). This probability is broadly peaked as the work function ϕ decreases, and decreases by approximately an order of magnitude when the velocity of the ions in the incident beam is decreased from 1.05×10^5 to 0.52×10^5 m s^{-1}, and the incident angle is $\theta_i=65°$ as measured from the surface normal. Theoretical calculations based on a many-body solution to the time-dependent Anderson-Newns model of charge transfer (discussed in the preceding paper) qualitatively reproduce the observed trends. These calculations suggest that the peak in the excited-state probability results mainly from two effects: first, the decreasing difference between the energy of the $Li^0(2p)$ state and the Fermi level as the work function decreases, which tends to increase the excited-state probability; and second, the competition of the $Li^0(2p)$ state with the $Li^-(2s^2)$ negative ion state at low work functions, which tends to decrease the excited-state probability. Differences between the $Li^0(2s)$ and $Li^0(2p)$ lifetimes also play a role in the formation of the peak, as does electron-hole pair production. [S0163-1829(96)08244-6]

I. INTRODUCTION

Charge transfer makes possible a number of outcomes when a positively charged ion collides with a surface, e.g., neutralization into ground or excited states, or the formation of negative ions. Thus, in an ion-scattering experiment, a variety of charge state species may be present in the scattered flux. In the preceding paper[1] (referred to hereafter as paper I), we saw that the dependence of the measured charge state fractions in the scattered flux could be qualitatively reproduced using a many-body model of resonant charge transfer, and we used the model to examine the detailed dynamics of the resonant charge-transfer process. We found that the dynamics were sensitive to the state of the ion-surface system when the ion is at its distance of closest approach to the surface, the energies of the atomic states relative to the Fermi level of the metal surface and to each other, and the lifetimes of the atomic states.

We can gain still more insight into charge-transfer dynamics by measuring other branching ratios, e.g., for excited-state formation. A thorough series of experiments by Kempter and co-workers[2–6] has shown that excited states of Li are formed during collisions of Li^+ ions with cesiated surfaces of tungsten. In these experiments the probability of $Li^0(2p)$ formation was found to have a broad peak as the surface work function was varied and a peak value of 0.10 or less. Such measurements of the work function and velocity dependence of the excited-state formation probability provide further tests for multiple-state charge-transfer models, and we will see that the observed dependences have their origins in the presence of multiple atomic states between which transitions can be made via the metal.

In this paper, we present measurements of the relative probability of formation of $Li^0(2p)$ when hyperthermal energy Li^+ ions collide with alkali-metal-covered Cu(001).[7,8] We then use these data to perform a detailed comparison with predictions obtained with the resonant charge transfer theory of Marston *et al.*[9] With the aid of the theoretical calculations, we can explain the trends in the data presented here and in the data of Kempter and co-workers. In particular, we develop a detailed explanation for the existence of the nonmonotonic dependence of the excited-state yield on surface work function that is seen in the alkali ion-surface systems. This dependence can only be explained using a multiple-state theory of charge transfer.

In Sec. II, we describe the experimental techniques for measuring the relative $Li^0(2p)$ yield. We present the data in Sec. III, and briefly describe the application of the theory in Sec. IV. We compare the predictions of the theory to the data in Sec. V, and conclude with a summary in Sec. VI.

II. EXPERIMENTAL TECHNIQUE

Our data were obtained in a versatile, two-tiered, ultrahigh vacuum (UHV) chamber that has been described elsewhere;[1,10] we provide relevant details here. The upper tier is devoted to preparing and monitoring the sample surface, and the lower tier is used for performing the ion-scattering measurements. The upper tier is equipped with a set of reverse-view optics for low energy electron diffraction, a set of optics for Auger electron spectroscopy (AES), a Kelvin probe, three alkali getter sources, and a sputter gun. The lower tier of the chamber contains the final electrostatic lens for focusing the ion beam onto the sample, a neutral

particle detector (NPD) for alkalis,[11,12] and a light collection system.[7,13]

A. Sample preparation

Before the measurements of the relative $Li^0(2p)$ formation probability were performed, both the orientation and the condition of the Cu(001) sample were checked as described elsewhere.[7] Our crystal cleaning procedure consists of Ar^+-ion sputtering and annealing.[1] The resulting surface was found to be clean to within the sensitivity of AES.

To change the work function of the surface, varying amounts of alkali were deposited with an outgassed commercially available getter source.[14] The procedure was discussed previously.[7] The work-function change $\Delta\phi$ of the sample surface was measured with the Kelvin probe. The uniformity and cleanliness of the alkali overlayers were checked with AES by preparing an overlayer, and then acquiring Auger spectra from different locations on the sample. The Auger spectra indicated a uniform coverage at all locations for both K and Cs overlayers, and that the overlayers were clean. The coverages achieved were $0<\theta_K<0.12$ and $0<\theta_{Cs}<0.14$, where θ_K (θ_{Cs}) is the K (Cs) coverage, and θ_K or $\theta_{Cs}=1$ corresponds to having one alkali adsorbate for every metal atom in the first layer of the surface. These coverages corresponded to work function changes $\Delta\phi=\phi_f-\phi_i$ of $0.0>\Delta\phi>-2.8$ eV for K and $0.0>\Delta\phi>-3.3$ eV for Cs, where ϕ_f (ϕ_i) is the final (initial) work function of the surface. We note that the geometric structures of the K and Cs overlayers in the respective coverage ranges given above are expected to be random.[15–19] During the measurements presented here, the pressure inside the UHV chamber was in the low 10^{-10}-torr range. This corresponds to a monolayer formation time of approximately 7 h if one assumes a sticking coefficient of unity. Thus we expect no significant residual gas adsorption to occur during our data acquisition, which takes no more than 30 min when measuring excited-state yields.

B. Detectors

The NPD is mounted on a rotating table whose axis of rotation coincides with the axis of the sample manipulator, as determined by an alignment procedure similar to that described by McEachern *et al.*[10] The operation and characteristics of the NPD have been described previously.[12]

The light detection system[7,13] consists of the collection optics, a set of filters, and a photomultiplier tube that was selected for its low dark count rate.[20] We checked for photon counts that may be due to the light emitted from the ion source or from fluorescence due to the chamber or other sources. We found none within the sensitivity of the light collection system. Finally, we found that greater than 90% of the detected light was due to the $Li^0(2p)\rightarrow Li^0(2s)$ transition for an incident beam energy of 400 eV. When K adsorbates were used to change the surface work function, light due to the $K^0(4p)\rightarrow K^0(4s)$ transition contributed a few percent or less of the detected light. We assume that the remainder of the detected light is due to transitions of higher excited states of Li. This assumption is supported by measurements of Andersson,[21] and also by the measurements of Schall *et al.*[4]

To measure the relative yield of $Li^0(2p)$, we used the following experimental sequence. The sample was prepared in the upper tier of the chamber by cleaning it and then depositing varying amounts of alkali; the resulting work function change $\Delta\phi$ was then measured. The beam current was then measured on the faceplate of a shielded Faraday cup.[22] After blocking the ion beam, the sample was moved to the lower tier of the vacuum chamber and placed into the path of the ion beam. The collection optics were then moved into position. The prepared sample was subsequently exposed to the beam, and photon counting would begin. After two sets of counting samples were obtained, the ion beam was prevented from entering the chamber and another (''background'') set of samples was obtained. Finally, the beam current was measured again in order to check the stability of the ion beam; the beam current varied no more than 5% during data acquisition. The entire sequence was repeated for different values of the work-function shift in order to produce the figures which are discussed in Sec. III.

Our detection scheme does not collect all of the photons emitted while the sample is exposed to the ion beam, nor does it distinguish among the trajectories of the atoms which emit detected photons. Therefore, a relative yield which is only a rough measure of the absolute yield is obtained. The interpretation of the relative yield is complicated by using alkali atom adsorption to change the surface work function and by the scattering geometry we employ. In particular, as more alkali adsorbates are added to the surface to lower the work function, the cross section for scattering increases. This is because the incident Li^+ ions can now strike adsorbates which may block those portions of the unit cell which would otherwise lead to implantation of the impinging ion. (If an extremely grazing scattering geometry can be utilized, as by Kempter *et al.*,[4] this effect is greatly reduced since most of the particles are reflected. For the experiments presented in this paper, we chose the incident angle to reduce the range of final velocities of the particles as much as possible without producing a false signal from collisions with other surfaces such as the tantalum retaining ring holding the sample in place). If the number of reflected ions increases and the probability for producing excited states remains constant, the observed photon count rate would increase. It would be incorrect to interpret such an increase as an increased probability for forming excited states.

To avoid the possibility of incorrectly interpreting changes in the photon count rate, we have used the neutral particle detector to measure intensity changes in the flux scattered into $\theta_f=65°$ relative to the surface normal to estimate the effect of alkali adsorbates on the scattering cross section. We found that the flux scattered from a surface with Cs adsorbates increased by approximately 15% with respect to scattering from the clean surface when $\theta_{Cs}=0.14$. By assuming that this same increase is achieved by the deposition of a K overlayer, that the increase is linear with $\Delta\phi$, and that this increase is the same for scattering into any final angle, we can crudely correct the data presented in Sec. III. There we will see that this correction produces only small changes in the work-function dependence of the relative yield. Thus we can interpret the overall qualitative work-function dependence of the relative yield to be the same as the relative probability of excited-state formation. We emphasize that the

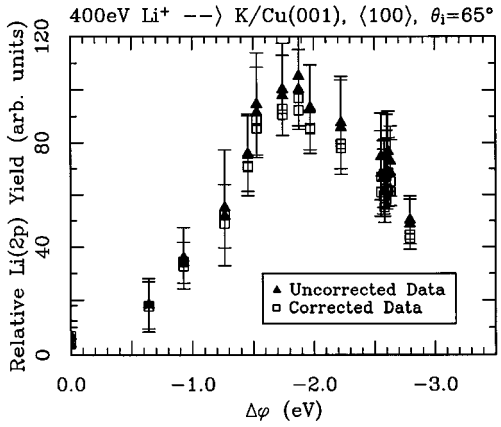

FIG. 1. The measured relative yield of $Li^0(2p)$ vs the work-function shift $\Delta\phi$ induced by depositing varying amounts of potassium. $E_i=400$ eV and $\theta_i=65°$. Open squares: data corrected by the increase in the fraction of scattered particles. Solid triangles: uncorrected data.

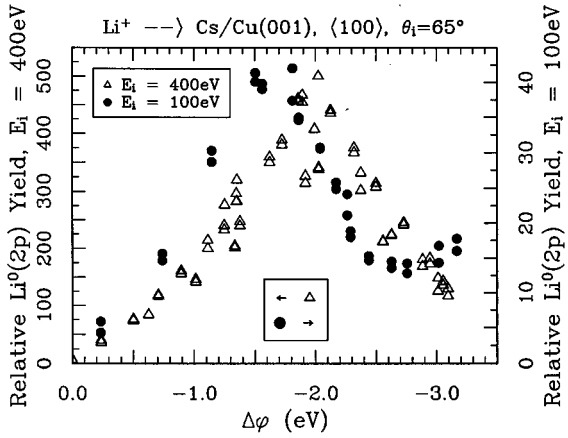

FIG. 2. The measured relative yield of $Li^0(2p)$ vs the work-function shift induced by depositing varying amounts of cesium. $E_i=400$ and 100 eV, and $\theta_i=65°$. Note the change of scale for the two different sets of data. Units for the vertical scales are arbitrary.

conclusions drawn in this paper do not depend on the small changes in the scattered intensity due to adsorbate scattering.

III. DATA

We measured the relative yield of atoms in the $Li^0(2p)$ state in the scattered flux versus the work-function change induced by the deposition of potassium when 400-eV Li^+ ions impinge on K/Cu(001) with $\theta_i=65°$ and along the $\langle 100\rangle$ azimuth; the results are shown as solid triangles in Fig. 1. Two data points are shown at each value of $\Delta\phi$ which correspond to the two consecutive sets of measurements taken as described in Sec. II B, and demonstrates that the effect of sample damage or adsorbate sputtering is small. By calculating the throughput of the collection optics, we *estimate* that the peak value of the relative yield corresponds to an absolute yield of 0.004 $Li^0(2p)$ atom per incident ion. We emphasize that this calculated yield is an estimate only.[23]

As expected from the one-electron picture, the yield of $Li^0(2p)$ in the scattered flux increases as $\Delta\phi$ decreases (i.e., as the work function decreases from the clean surface value). However, the yield achieves a maximum value at $\Delta\phi\approx-2.0$ eV ($\phi=2.59$ eV), and then decreases as $\Delta\phi$ further decreases. The observed nonmonotonic behavior cannot be explained with the one-electron picture of charge transfer for a single state, which was useful for understanding the trends in the positive and negative ion survival probabilities.[1] To understand the behavior of the $Li^0(2p)$ yield, one must consider multiple-state charge transfer models.

As mentioned in Sec. II, we can correct the data in Fig. 1 for the effect of the increasing scattering cross section. We see that the dependence of the corrected data, shown as open squares, has essentially the same ϕ dependence seen in the raw data. Because of this, and the crude nature of the correction, the data presented hereafter are not corrected for the increase in the scattering cross section.

The relative yield of $Li^0(2p)$ versus the work-function change induced by the deposition of cesium is shown in Fig. 2 for incident energies of 400 and 100 eV. Here the Li^+ ions impinge on the Cs/Cu(001) surface with an incident angle $\theta_i=65°$ and along the $\langle 100\rangle$ azimuth. As the work function decreases, the relative yields for both incident energies increase, pass through a maximum, and then decrease. This behavior is similar to that obtained using K overlayers, and is similar to the behavior observed by Kempter and co-workers for $Li^+\rightarrow$ Cs/W(110).[4,5] We estimate that the peak values of the relative yields correspond to absolute yields of 0.004 $Li^0(2p)$ atom per incident ion when $E_i=400$ eV, and 0.0003 $Li^0(2p)$ atom per incident ion when $E_i=100$ eV.

By changing the incident energy from $E_i=400$ eV to $E_i=100$ eV, we change the time that the ion spends in the vicinity of the surface. Thus we change the time scale associated with the motion of the ion. This produces two effects as the incident energy is decreased: first, the yield of atoms in the $Li^0(2p)$ state decreases by approximately an order of magnitude; second, the peak in the yield shifts to larger work-function values. We also note that the data for $E_i=100$ eV show a small increase at the lowest work functions. We will discuss how these observations can be explained in the following sections.

IV. THEORY

To interpret the data presented in Sec. III in detail, we use the model of Marston *et al.*[9] as described in paper I. Briefly, the model consists of an atom interacting with a metal as described by a generalized version of the Anderson-Newns Hamiltonian.[24] Transitions can be made between the atomic states via the metal, and the corresponding transition rates decrease as the distance z between the metal and the atom is increased. The rate of decrease with z is different for the different atomic states; the states with more spatially extended orbitals have transition rates that decrease relatively slowly with distance. For example, the transistion rate between the $Li^0(2p)$ state and the metal decreases with z more slowly than that between the $Li^0(2s)$ state and the metal. Since the transition rates are similar when z is small,[25] the transition rate for $Li^0(2p)$ is always larger than that for $Li^0(2s)$. Input to the calculation of the charge state fractions

are the energies and lifetimes of the participating atomic states, the normal velocity of the particle, the density of states of the metal, and the work function of the surface. We will use the same values for these quantities as in paper I.[1] All of the calculations begin with the atom at $z=1$ Å with the ion-surface system in its ground state. Because the couplings between the atomic states and the metal are quite large for that value of z, the ground state is a hybrid of the basis states[1] used to solve the Schrödinger equation. Thus basis states of higher energy than the lowest-energy basis state can have appreciable occupancies at $z=1$ Å [e.g., the occupancy of the $Li^0(2p)$ state can be appreciable, even though the $Li^0(2s)$ state is always of lower energy].

Here we explain how we have applied the model to describe the data. Recall that the measurement of the relative $Li^0(2p)$ yield (i.e., the photon count rate) does not identify the trajectory of the atom that emitted the detected photon corresponding to the $Li^0(2p)\rightarrow Li^0(2s)$ transition. Thus atoms scattered into *any* final angle can emit photons that reach the detector. In principle, it is therefore necessary to measure the energy and angular distributions (from which one can derive the velocity distributions) of the scattered atoms and use these together with the calculated velocity dependence of the excited-state formation probability to obtain yields that can be compared to the measured yields. We have measured the in-plane energy and angular distributions,[26] and have derived the corresponding normal velocity distribution.[27] By using the model to calculate the excited-state probability as a function of normal exit velocity, we found that lithium particles scattered into a final angle of $\theta_f \approx 0°$ (which have the greatest normal velocity) have a probability of surviving the ion-surface collision in the $Li^0(2p)$ excited state which is roughly three orders of magnitude greater than for particles scattered into the rainbow angle ($\approx 76°$).[27] We also found that the intensity scattered into the rainbow angle is only approximately ten times greater than that scattered into $\theta_f \approx 0°$. Therefore, for the purpose of making qualitative comparisons, it is sufficient to assume that only those particles leaving the surface with the highest normal velocity contribute significantly to the corresponding photon flux that was measured. For $E_i=400$ eV, particles scattered in plane and into $\theta_f=0°$ had a normal velocity of $v_z=0.89\times10^5$ m s^{-1} ($v_z=0.04$ a.u.), while for $E_i=100$ eV, the final normal velocity was $v_z=0.44\times10^5$ m s^{-1} ($v_z=0.02$ a.u.).

It is therefore possible to compare the theoretical results obtained by assuming a single velocity (corresponding to the largest final normal velocity attained by particles in the scattered flux) to the data. This is why we did not weight the theoretical calculations by measured velocity distributions before comparing the theory to the data.

V. DISCUSSION

The measured excited-state yields provide further information against which charge-transfer theories must be tested. The observations of excited states in the scattered flux are particularly interesting since they cannot be explained by a theory which considers only a single state; these observations require that we consider multiple states. In this section, we give explanations for the trends seen in the calculated excited-state yields. Comparison of the calculated trends to the measured trends, together with careful examination of the calculated trends, helps us obtain a more detailed picture of the dynamics of charge transfer.

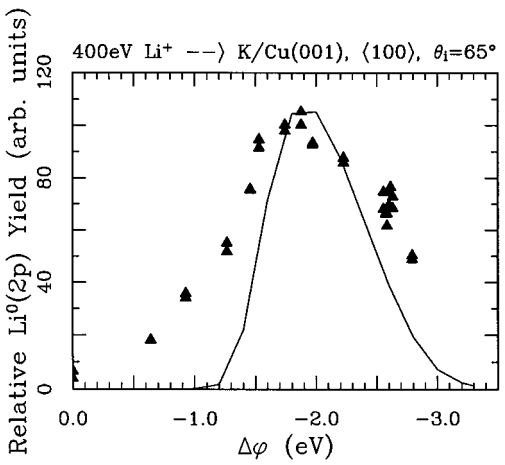

FIG. 3. Comparison of the calculated probability for forming $Li^0(2p)$ to the measured relative $Li^0(2p)$ yield for 400-eV Li^+ incident on K/Cu(001). The calculated curve is normalized to the data. Solid triangles: measured relative $Li^0(2p)$ yield. Solid line: $P^0(2p)$, calculated using the four-parameter functions to fit the resonance widths calculated by Nordlander.

We now briefly review some of the findings obtained by examining a large number of calculations.[1] First, the initial state of the system when the ion is close to the surface (recall that every calculation in this paper starts with the atom close to the surface) plays a large role in determining the final occupations. Second, energies of the atomic states relative to the Fermi level of the metal are important; it is often true that a significant amount of charge is exchanged between the metal and an atomic state in the vicinity of the Fermi-level crossing for that state. Third, the relationship between the time scales set by the resonance widths (i.e., the many-body couplings) and the velocity of the scattered particle partly determines the amount of charge transferred during a scattering event. It is necessary to keep *all three* of the above findings in mind when explaining the trends in the measured branching ratios.

A. Overview

In Fig. 3, the calculated work function dependence of the probability for scattering into the $Li^0(2p)$ state, $P^0(2p)$, is shown and compared to the measured relative $Li^0(2p)$ yield from Fig. 1. We see that the model predicts a peak in $P^0(2p)$ at $\Delta\phi \approx -1.9$ eV, which is approximately the same as that for the measured peak (≈ -2.0 eV). The peak value of the calculated probability is normalized to the peak value of the measured yield. We note that the peak value of the measured yield is estimated to be 0.004, while the calculated value is 0.021.

An explanation of the origin of this peak is as follows. First, we consider how the initial state of the ion-surface system (i.e., the system in its lowest-energy state with the particle at its distance of closest approach to the surface) changes as the work function decreases. As can be seen in

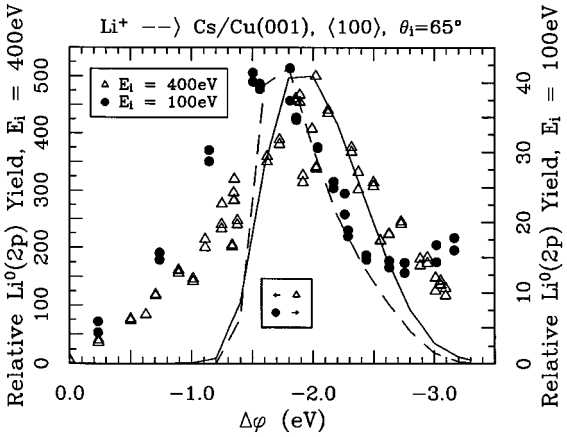

FIG. 4. Comparison of the calculated probability for forming $Li^0(2p)$ to the measured relative $Li^0(2p)$ yield for 400- and 100-eV Li^+ incident on Cs/Cu(001). Each calculated curve was normalized to the relevant data set. The calculations were done using the four-parameter functions to fit the resonance widths calculated by Nordlander. Note the change in the vertical scale for the two sets of data.

Fig. 7 of paper I, the calculated initial occupancy of the $Li^0(2p)$ state is about 0.10 at $z=1$ Å for $\phi=4.59$ eV ($\Delta\phi=0.00$ eV); this increases to 0.14 as the work function is decreased to $\phi=2.79$ ($\Delta\phi=-1.8$ eV). As the work function decreases further, the initial occupancy of the $Li^0(2p)$ state decreases rapidly due to the fact that the negative ion state becomes the lowest energy state near the surface.[1] Now we consider the charge transfer dynamics on the outgoing trajectory. For high work functions, the $Li^0(2p)$ state does not cross the Fermi level; therefore its initial occupancy decays essentially to the $Li^0(2s)$ state via the metal as the atom moves away from the surface. As the work function is decreased, eventually the $Li^0(2p)$ state just crosses the Fermi level (at large z); therefore, although the initial occupancy again decays as the atom moves away from the surface, it recovers some occupancy after crossing the Fermi level. Occupancy remains in the $Li^0(2p)$ state if it was obtained far enough from the surface that the $Li^0(2s)$ state is only weakly coupled via the metal to the $Li^0(2p)$ state. As the work function is decreased further, the $Li^0(2p)$ state loses occupancy even more rapidly on the outgoing trajectory due to the increasing importance of the negative ion state. Thus $P^0(2p)$ achieves a maximum at intermediate work-function values.

Another feature to note in Fig. 3 is that the measured curve is much more broad than the theoretical curve. We attribute this to the effect of variations in the local electrostatic potential induced by the K adsorbates, as has been discussed previously[28–35] and in paper I.

Recall from Fig. 2 and the associated discussion that there is roughly an order-of-magnitude difference between the peak values of the relative $Li^0(2p)$ yields measured for $E_i=100$ and 400 eV. In Fig. 4, we present a comparison of calculated $Li^0(2p)$ yields to the measured relative $Li^0(2p)$ yields obtained when using cesium adsorbates (the theoretical curve for $E_i=400$ eV is identical to that in Fig. 3). The theoretical curves are normalized to the peak values of the appropriate experimental curves. The ratio of these measured peak values is 0.075. However, it is likely that the scattering cross section for $E_i=100$ eV is somewhat larger than for $E_i=400$ eV, which would reduce the value of this ratio. For comparison, the ratio of the calculated peak values is 0.080. A simple explanation for the decrease in the magnitude is that, for a given work function, the adiabatic charge state [i.e., the $Li^0(2s)$ state] occupancy increases as the exit velocity of the particle is decreased since the system has more time to evolve into the adiabatic state.

As noted above, the peaks in the measured relative yields for $E_i=400$ and 100 eV, shown in Fig. 2, are shifted with respect to one another. For $E_i=400$ eV, the calculated peak in Fig. 4 occurs at $\Delta\phi\approx-1.9$ eV, which closely matches the observed peak at $\Delta\phi\approx-2.0$ eV. For $E_i=100$ eV, the calculated peak occurs at $\Delta\phi\approx-1.7$ eV, close to the observed value of $\Delta\phi\approx-1.6$ eV. Thus the direction of the observed $P^0(2p)$ peak shift is reproduced by the calculations.

The shift of the calculated peak in $P^0(2p)$ is due to a combination of effects: the work-function dependence of the initial occupancy of the $Li^0(2p)$ state (recall Fig. 7 of paper I), the change in the velocity, and the decrease in the Fermi-level crossing distance for the $Li^0(2p)$ state with decreasing work function. Consider the following: the higher the velocity, the more one expects that the peak in $P^0(2p)$ will occur at the same work-function value as the peak in the initial occupancy ($\phi=2.79$ eV, or $\Delta\phi=-1.8$ eV), which approximately occurs when the Fermi level and the $Li^0(2p)$ state are degenerate at the surface ($z=1$ Å). As the velocity decreases, however, the occupancy of the $Li^0(2p)$ state has more time to decay while the atom is pulled away from the surface, and thus the final occupancy will more strongly reflect the occupancy that is recovered upon crossing the Fermi level. To ensure that the largest $Li^0(2p)$ occupancy is recovered, the Fermi-level crossing for the $Li^0(2p)$ state must occur at a distance a little beyond that at which transitions between the metal and the $Li^0(2s)$ state have essentially ceased [this prevents the decay of the $Li^0(2p)$ occupancy via transistions to the metal and subsequently to the $Li^0(2s)$ state]. For high and intermediate work-function values, this distance is roughly $z=4$–5 Å. This range of distances corresponds [via the energy of the $Li^0(2p)$ state] to a range of work functions between $\phi=2.7$ and 2.9 eV. Thus we see that, at higher velocity, the peak in $P^0(2p)$ occurs near the work function value for which the maximum initial occupancy of the $Li^0(2p)$ state is attained; at lower velocity, the peak occurs at a work function value corresponding to a larger Fermi level crossing distance for the $Li^0(2p)$. This is why the calculated peak in $P^0(2p)$ is shifted to higher work function as the final normal velocity is decreased from $v_z=0.04$ to $v_z=0.02$ a.u.

We investigated whether the trends in the calculated $P^0(2p)$ (i.e., the existence of a peak in the work function dependence, the decrease in the peak values with velocity, and the shift of the peak value) vary with the magnitudes of the resonance widths, the rates at which the resonance widths change with distance, the relative magnitudes of the resonance widths, and the initial occupancies of the different basis states. We found that the qualitative trends in the calculated $Li^0(2p)$ yield shown in Figs. 3 and 4 are robust if

these quantities are varied within reasonable limits. By increasing or decreasing the magnitude of all of the resonance widths by a factor of 2, a peak in the work function dependence of $P^0(2p)$ is still obtained. The work function at which the peak value of $P^0(2p)$ occurs shifts slightly, and the peak values increase as the resonance widths are all increased. Having established that the trends in the calculated trends are robust, we now turn to the details of the charge transfer dynamics and the origins of the peak in the work function dependence of the excited state yield.

B. Details of the dynamics

In the previous subsection, we discussed how the peak in the excited-state yield exists in large part due to the changing energetics of the system as the work function is changed. That the initial occupancy of $Li^0(2p)$ decreased in part due to the increasing occupancy of the negative ion state for low work-function values suggests that other states of the system may also play a role in determining the work function dependence of $P^0(2p)$. To increase our understanding of the role of the $Li^-(2s^2)$ state and of the other states (the positive ion state, the positive ion state with an electron-hole pair, and the neutral ground state and excited atom states) in producing the peak in $P^0(2p)$, we examined the predictions of the model in detail. We systematically removed different states from the model to see if the peak in $P^0(2p)$ persists after their removal, thereby checking if their presence plays a role in the peak formation. Since we expect the relative energies and lifetimes of these states to play an important role in the formation of the peak, we also investigated the dependence of $P^0(2p)$ on these parameters.

By performing a number of calculations, we found conditions that are sufficient to produce the peak in the calculated work function dependence of $P^0(2p)$. For example, as described above, competition of the $Li^0(2p)$ state with the negative ion state plays a major role in the production of the peak in $P^0(2p)$. Also, the production of electron-hole pairs influences the work function dependence of $P^0(2p)$. We also found that the difference between the resonance widths of the $Li^0(2p)$ state and $Li^0(2s)$ state can, under certain conditions, produce a peak in $P^0(2p)$. We discuss these results in more detail in the following subsections.

1. Explanation of the nonmonotonic behavior of $P^0(2p)$

(a) Removal of the $Li^-(2s^2)$ state. We checked the idea that the $Li^-(2s^2)$ state competes with the $Li^0(2p)$ state by effectively removing the negative ion state from the calculation (we do this by making it energetically very unfavorable for the negative ion to form). The resulting dependence of $P^0(2p)$ on $\Delta\phi$ is shown in Fig. 5 as the dashed–double-dotted line (compare to the calculation in which all states are included, shown as the solid line). We see that removing the negative ion state does not destroy the peak in $P^0(2p)$, and slightly changes the surface work function value at which $P^0(2p)$ achieves its maximum.

The main differences are that the magnitude of the final peak value of $P^0(2p)$ has increased to 0.052 (from 0.021, when all states are included), and that the dependence on $\Delta\phi$ has changed [specifically, at the lowest work functions, $P^0(2p)$ does not approach zero]. Since removing the negative ion state does not destroy the peak in $P^0(2p)$, its presence is not necessary to form the peak, i.e., it is not necessary to include the negative ion state in the calculation to produce a maximum in the work function dependence of $P^0(2p)$. However, the negative ion state does play a role in the dynamics. The fact that the peak value of $P^0(2p)$ increases upon removing the negative ion state is consistent with the idea that the negative ion state competes with the $Li^0(2p)$ state for electrons in the metal. The increase in $P^0(2p)$ can be traced, in part, back to the increase of the initial occupancy of the $Li^0(2p)$ state that results from the elimination of the negative ion state. The initial value of $P^0(2p)$ with $\phi = 2.59$ eV, and the negative ion state removed, is increased by an amount 0.045 (with respect to the calculation in which all states are included), which is larger than the difference $(0.052 - 0.021 = 0.031)$ in the final $P^0(2p)$ peak values; this shows that the evolutions of the occupancies are changed by the absence of the negative ion state.

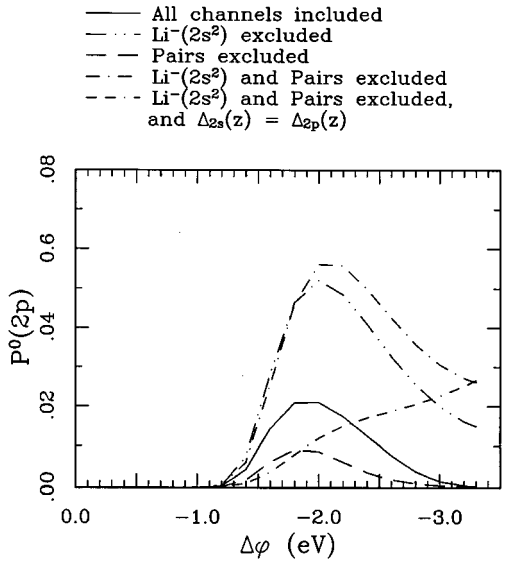

FIG. 5. Calculated dependence of $P^0(2p)$ on $\Delta\phi$ when excluding different channels. Here the four-parameter functions are used to fit the resonance widths calculated by Nordlander.

We conclude that the negative ion state provides an additional channel which can take occupancy away from the $Li^0(2p)$ state when the particle is close to the surface. The presence of the negative ion state not only affects the initial value of $P^0(2p)$ but also changes the dynamics (which depend on the instantaneous occupancies), especially for the low work functions at which negative ions are formed. Thus the negative ion state is important in determining the yield of atoms which scatter from the surface in excited electronic states.

(b) Removal of the pair state. We similarly investigated the effects on the dynamics of removing the electron-hole pair state from the calculation; this prevents transitions between the $Li^0(2s)$ state and the $Li^0(2p)$ state via the formation of an electron-hole pair. In this case, which is illustrated by the dashed line in Fig. 5, the peak in $P^0(2p)$ persists and is slightly shifted toward higher work-function values. The peak value is 0.009, less than half that obtained when all states are included in the calculation. The peak shape does

not change appreciably. These results show that the pair state is not necessary for the formation of the peak in $P^0(2p)$ versus work function, but it does affect the calculated final yields. Examining the evolution of the occupancies for several different work functions, we find that the exclusion of the pair state results in very little difference at the highest work functions [corresponding to the clean Cu(001) surface, i.e., $\phi = 4.59$ eV]. However, at intermediate and low work functions, the exclusion of the pair state leads to an increased occupation of the negative ion state. This is because there is no longer any occupancy in the pair state that can flow to the $Li^0(2p)$ state [simply put, we reduced the number of ways in which the $Li^0(2p)$ state can obtain occupancy by removing the pair state]. Therefore, probability which would have flowed to the $Li^0(2p)$ state effectively goes to the negative ion state.

(c) Removal of the $Li^-(2s^2)$ and pair states. For completeness, it is interesting to look at the behavior of the occupancies when both the negative ion state and the electron-hole pair state are removed from the calculation. As shown in Fig. 5, removing these states from the calculation does not destroy the peak, and the peak is shifted to slightly lower work functions. The peak value of $P^0(2p)$ is more than twice as large (0.056 compared to 0.021 when all states are included in the calculation), and the peak shape differs at the lower work functions. This shows that the combined presence of the negative ion state and the pair state is not necessary to produce the peak in $P^0(2p)$. The increase in the final peak value, the shift of the peak and its change of shape at low work functions is mainly due to the exclusion of the negative ion state.

(d) Removal of the $Li^-(2s^2)$ and pair states, with $\Delta_{2p}(z) = \Delta_{2s}(z)$. Clearly, attributing the existence of the peak solely to competition with either the negative ion state, the pair state, or the combination of the two is incorrect although these states (especially the negative ion state) certainly affect the dynamics of the charge transfer. We are therefore led to hypothesize that the energies and lifetimes of the $Li^0(2s)$ and $Li^0(2p)$ states alone can be enough to produce the peak. To test this hypothesis, we performed a calculation for which the $Li^0(2p)$ resonance width is set equal to the usual $Li^0(2s)$ resonance width [i.e., $\Delta_{2p}(z) = \Delta_{2s}(z)$] when both the negative ion and pair states are removed from the calculation. The result, shown in Fig. 5 as the double-dash–dotted line, is that the peak in $P^0(2p)$ is destroyed by setting the resonance widths equal to one another.

We investigated this result by comparing the evolution of the $Li^0(2p)$ occupancy at different work-function values. In Fig. 6, we show how $P^0(2p)$ varies with distance for a number of work-function values when the negative ion and pair states are removed and $\Delta_{2p}(z) \neq \Delta_{2s}(z)$. We show the corresponding series of curves for the case in which the negative ion and pair states are removed and $\Delta_{2p}(z) = \Delta_{2s}(z)$ in Fig. 7. We see that when $\Delta_{2p}(z) \neq \Delta_{2s}(z)$, $P^0(2p)$ decreases less rapidly with z than when $\Delta_{2p}(z) = \Delta_{2s}(z)$. [Recall that, as the system evolves in time, it strives for the ground state, which, even fairly close to the surface, is essentially the $Li^0(2s)$ state, so $P^0(2p)$ decreases.] Additionally, we find that $P^0(2p)$ passes through a minimum and increases somewhat for intermediate work-function values when $\Delta_{2p}(z)$

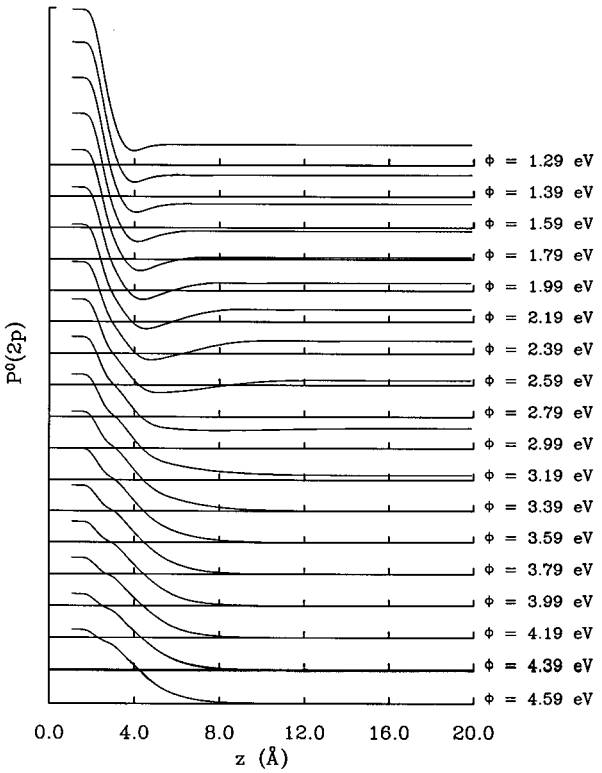

FIG. 6. Calculated dependence of $P^0(2p)$ when excluding the negative ion and pair states, using the four-parameter functions to fit the resonance widths calculated by Nordlander, for different work functions. Here $\Delta_{2p}(z) \neq \Delta_{2s}(z)$.

$\neq \Delta_{2s}(z)$. This increase is much reduced when $\Delta_{2p}(z) = \Delta_{2s}(z)$.

We now give an intuitive explanation for the behavior described immediately above for the case in which $\Delta_{2p}(z) \neq \Delta_{2s}(z)$. First, recall that each calculation of the occupancies begins at $z = 1$ Å, with the ion-surface system in its ground state (hybrid of basis states). At the highest work-function values, the $Li^0(2p)$ state lies essentially above the Fermi level, and so it will not be occupied far from the surface. As the work function decreases, the $Li^0(2p)$ state eventually just crosses the Fermi level (at large z). As the work function decreases a bit more, the Fermi-level crossing distance for the $Li^0(2p)$ state decreases, but is still greater than the distance at which electron hopping between the states of the metal and the $Li^0(2s)$ state has essentially ceased. Thus, during the outgoing trajectory, the $Li^0(2p)$ state can fill without losing occupancy to the energetically favored $Li^0(2s)$ state. This leads to the increase of $P^0(2p)$ at moderate values of z for intermediate work-function values in Fig. 6. As the work function is decreased still further, the Fermi-level crossing for the $Li^0(2p)$ state occurs at z values for which electron hopping to and from the $Li^0(2s)$ state still occurs. Therefore the $Li^0(2p)$ state can now lose occupancy to the $Li^0(2s)$ state, and the final occupancy of $Li^0(2p)$ is decreased. According to this simple picture, we expect that the peak in the $Li^0(2p)$ yield will occur at a work function value for which the Fermi-level crossing of the $Li^0(2p)$ state is just beyond the distance at which hopping from the $Li^0(2s)$ state ceases, or about $z = 6$ Å. This

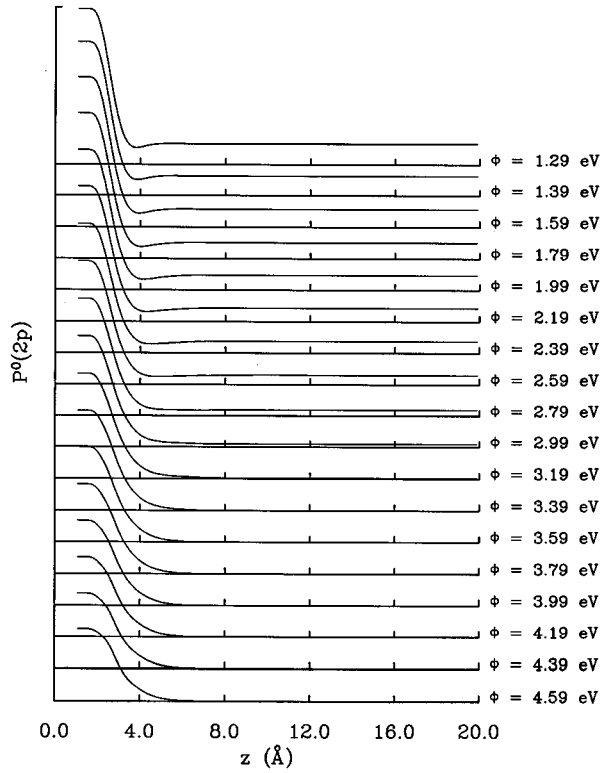

FIG. 7. Calculated dependence of $P^0(2p)$ when excluding the negative ion and pair states, using the four-parameter functions to fit the resonance widths calculated by Nordlander, for different work functions and $\Delta_{2p}(z)=\Delta_{2s}(z)$.

corresponds to a work-function value of about 3 eV, or $\Delta\phi=-1.6$ eV, which is to be compared to the measured value of $\Delta\phi=-2.0$ eV. Although the above explanation (based solely on *energetics* within a one-electron picture) is useful for a *qualitative* understanding of the existence of the peak, it cannot be used to make quantitative predictions, since the dynamics of the system also depend on the velocity of the scattered particle.

For the case in which $\Delta_{2p}(z)=\Delta_{2s}(z)$, electron hopping between the states of the metal and *both* the $Li^0(2s)$ and $Li^0(2p)$ states ceases simultaneously. Therefore, the $Li^0(2p)$ state does not gain much occupancy when passing through the Fermi level, and hence $P^0(2p)$ does not recover at moderate z as much as when $\Delta_{2p}(z)\neq\Delta_{2s}(z)$, as seen in Fig. 7.

What is the property of the $Li^0(2p)$ resonance width that causes the existence of the peak in $P^0(2p)$? Is it sufficient for the $Li^0(2p)$ resonance width to have a different magnitude than the $Li^0(2s)$ resonance width, or is it necessary to have a different distance dependence? To find the answer, we used the model to calculate the effect of changing Δ_0 when the parameter α (see paper I, Table II) was set to be the same for $\Delta_{2p}(z)$ and $\Delta_{2s}(z)$. We found that, when both the negative ion and pair states had been eliminated from the calculation, the peak in $P^0(2p)$ is destroyed as long as α is the same for the $Li^0(2s)$ state and the $Li^0(2p)$ state. We conclude that in order for the peak in $P^0(2p)$ to survive in the special case where the negative ion and pair states are removed, it is necessary for α to be different; i.e., it is necessary that the *rates* at which the $Li^0(2s)$ and $Li^0(2p)$ resonance widths decay with distance from the surface be different. These rates are different because the $2s$ and $2p$ orbitals of Li have different spatial extents. Thus, for the special case in which the negative ion and electron-hole pair states are excluded, the existence of the peak is intimately related to the spatial extents of the $Li^0(2s)$ and $Li^0(2p)$ orbitals. We note that the above condition is not always sufficient to remove the peak seen in $P^0(2p)$. For example, if $\Delta_{2s}(z)=\Delta_{2p}(z)$ but the negative ion state is included, the peak in $P^0(2p)$ is recovered.

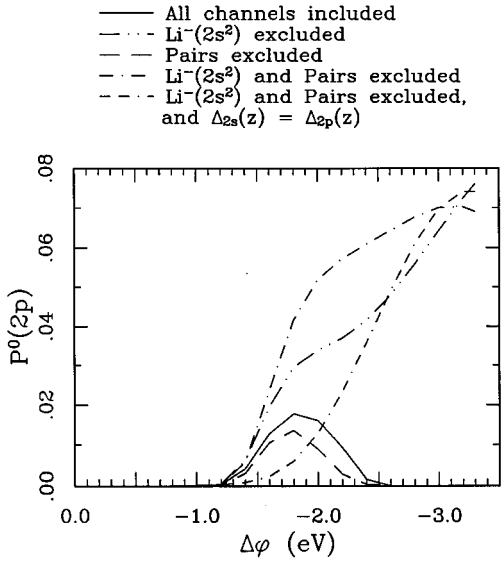

FIG. 8. Calculated dependence of $P^0(2p)$ on $\Delta\phi$ when excluding different channels. Here the resonance widths used to generate Fig. 5 have been halved.

(e) Dependence on the magnitudes of the atomic state lifetimes. We performed further simulations to determine if the above conclusions are sensitive to changing all of the resonance widths by factors of 2. The results are shown in Figs. 8 and 9 for the cases in which the resonance widths are decreased by a factor of 2 and increased by a factor of 2, respectively. We find that when the resonance widths are decreased by a factor of 2, we obtain behavior different from that shown in Fig. 5 when excluding various channels from the calculation. This is due to the fact that the resonance widths are now small enough that transitions between the states (via the metal) are significantly hindered. It may be that using resonance widths this narrow prevents memory loss, since the results become even more dependent on the initial state. When the resonance widths are increased by a factor of 2, however, similar effects due to eliminating the different states are seen. We remind the reader that the single particle widths are merely *suggested* input for the theory of Marston *et al.* We note that Sulston, Amos, and Davison used narrow widths which have the same rate of decay (i.e., the same value of α) and found no peak in $P^0(2p)$.[36]

2. Sensitivity of calculated trends to atomic state lifetimes

We investigated trends in the calculated excited-state yields and how these trends depend on a number of quanti-

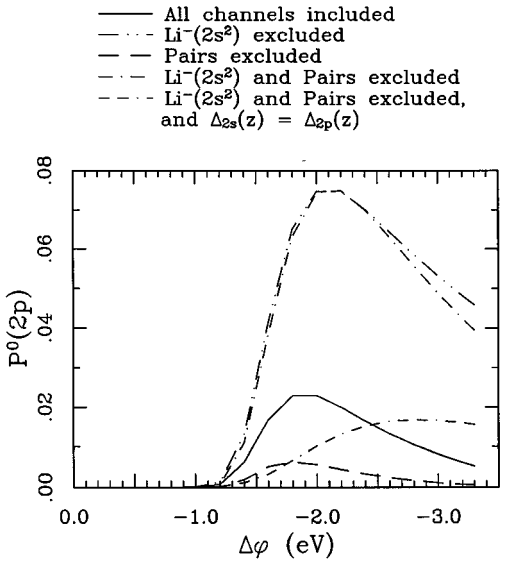

FIG. 9. Calculated dependence of $P^0(2p)$ on $\Delta\phi$ when excluding different channels. Here the resonance widths used to generate Fig. 5 have been doubled.

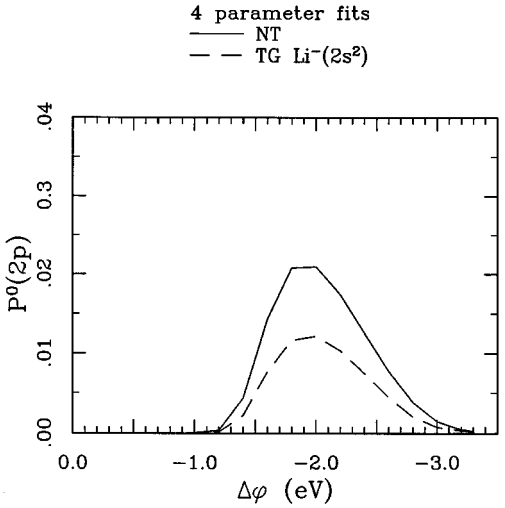

FIG. 11. Calculated $P^0(2p)$ vs $\Delta\phi$ using the negative ion state resonance widths calculated by Nordlander and by Teillet-Billy and Gauyacq.

ties which are input to the model. We began by varying the magnitudes of all of the resonance widths (i.e., the lifetimes) of the atomic states.

The value of $\Delta\phi$ at which the peak value of $P^0(2p)$ occurs changes somewhat if we change the resonance widths of all of the atomic states. We illustrate this in Fig. 10, which is a plot of $P^0(2p)$ versus $\Delta\phi$ using different resonance widths. We see that, in changing the widths by a factor of 4, the position of the peak changes by approximately 0.1 eV. Also, the peak value increases when all of the resonance widths are increased.

We also checked the dependence of other trends in the calculated excited yields on the magnitude of the resonance widths. We found that the direction of the peak shift with decreasing ion velocity is insensitive to decreasing or increasing the resonance widths by a factor of 2. We also found that the magnitude of the peak value of $P^0(2p)$ decreases with decreasing velocity when decreasing or increasing the resonance widths by a factor of 2. Also, the ratio of the peak values obtained for $v_z=0.02$ and $v_z=0.04$ a.u. range between 0.07 and 0.12 when decreasing or increasing the resonance widths by a factor of 2 (recall that the measured value is 0.075).

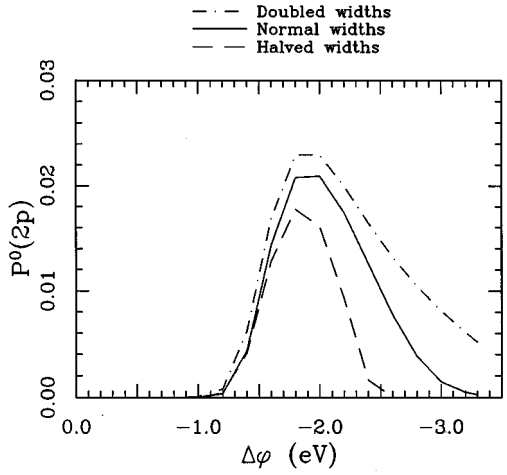

FIG. 10. Calculated $P^0(2p)$ vs $\Delta\phi$ using resonance widths that differ by factors of 2. Here, the four-parameter functions are used to fit the resonance widths calculated by Nordlander.

We also varied the relative magnitudes of the resonance widths by using the negative ion state resonance width calculated by Teillet-Billy and Gauyacq (this width is larger than that calculated by Nordlander and Tully, because polarization of the atom by the surface potential is included). We compare this to the result obtained by using the negative ion state resonance width calculated by Nordlander in Fig. 11. We see that the peak value of $P^0(2p)$ has decreased by about a factor of 2, and that the peak has hardly shifted. The decrease in the peak value is due to the increased coupling (via the metal) of the $Li^-(2s^2)$ state to the $Li^0(2s)$ state. The increased coupling serves to increase the negative ion state occupancy in the vicinity of the surface for high and intermediate work functions ($\phi=4.59-3.22$ eV) since the negative ion state is not the lowest energy-basis state. The increased coupling also essentially increases the rate at which occupancy can be drained away from the $Li^0(2p)$ state [via the metal to the $Li^0(2s)$ state]. This leads to the more rapid decrease in occupancy of the $Li^0(2p)$ state over the same spatial range, which results in smaller final values of $P^0(2p)$. It is important to note that changing the relative magnitudes of the resonance widths by a moderate amount does not destroy the peak seen in the $P^0(2p)$ dependence.

To conclude our discussion, we ask which occupied states of the metal are most likely to transfer an electron into the $Li^0(2p)$ state. To answer this question, in Fig. 12 we plot the calculated probability of creating a hole in the metal which is associated with producing a $Li^0(2p)$ atom versus both the energy of the hole and the distance z of the lithium atom from the surface. In this figure, $\phi=2.79$ eV ($\Delta\phi=-1.8$

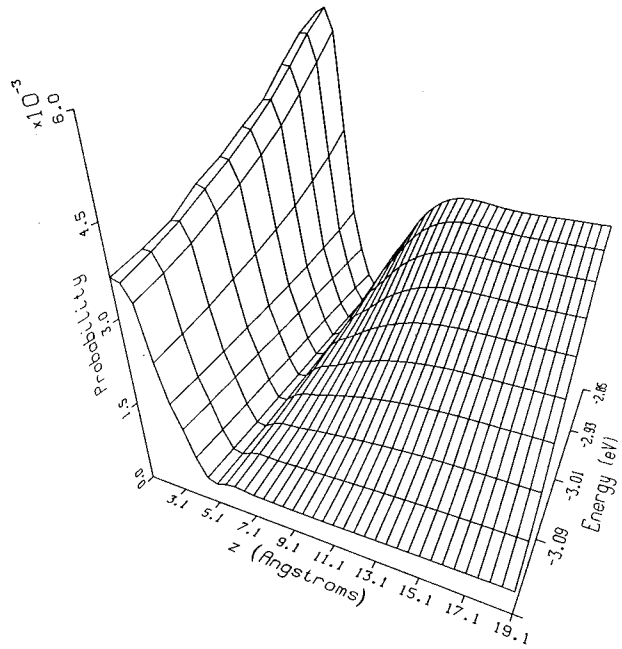

FIG. 12. Calculated probability for leaving a hole behind in the metal in order to make $Li^0(2p)$, vs the energy of the hole and vs z. The four-parameter functions are used to fit the resonance widths calculated by Nordlander, and $\phi = 2.79$ eV ($\Delta\phi = -1.8$ eV). Here, the zero of energy is the vacuum, and the Fermi level is at -2.79 eV. In the numerical solution of Marston *et al.*, the highest occupied state of the metal is at -2.81 eV; the next nine lower states (each separated from the previous one by -0.04 eV) are also shown.

eV), and only the first ten states of the metal below the Fermi level (they are separated by 0.04 eV) are shown. We find that, close to the surface ($z = 1$ Å), the states near the Fermi level have about the same occupancy. Their initial occupancies rapidly decrease as z increases to about 4.5 Å. As z continues to increase, a few states closest to the Fermi level are mostly responsible for the final population of the $Li^0(2p)$ state. This is simply because the transition rate is largest at the Fermi level.

3. Alternative explanation of the nonmonotonic behavior of $P^0(2p)$

Kempter and co-workers previously observed a peak in the $Li^0(2p)$ formation probability for 1-keV Li^+ incident on Cs/W(110) at grazing incident angles.[4,5,37] The mechanism proposed for the peak observed in that system is as follows.[4,37] First, an electron from the surface is resonantly transferred into the $Li^0(2p)$ state of the atom during the approach of the incoming ion to the surface. The resultant excited atom then makes a transition to the ground state through the mechanism of Auger deexcitation. The neutral atom then makes a hard collision with the surface, during which the $Li^0(2p)$ state is again populated due to the hybridization of the atomic orbitals. Finally, the resulting excited atom must then survive both Auger deexcitation and resonant ionization in order to emit a photon that is detected. Thus, Kempter and co-workers suggested that the peak in their data is due to the changing relative importance of Auger deexcitation and resonant ionization as the work function of the surface is altered. That Auger deexcitation occurs in this system has been verified by measurements of electron energy spectra[37,38] which have intensity peaks that can be attributed to the deexcitation of the following excited states of lithium: $Li^0(2p)$, $Li^0(3s)$, $Li^0(3p)$, and $Li^0(3d)$. The lithium $n=3$ states may deexcite to either the $Li^0(2s)$ ground state or to the $Li^0(2p)$ state.

We have seen above that it is not necessary to invoke Auger deexcitation during the *outgoing* trajectory in order to obtain a peak in the relative probability of $Li^0(2p)$ formation versus the work-function change $\Delta\phi$. It is possible to account for most of the measurements (that is, the measurements presented in this paper and those reported by Kempter and co-workers) by assuming that Auger deexcitation occurs during the incoming trajectory and that the resonant mechanism is the dominant charge-transfer process during the outgoing trajectory. It is important to note that we are assuming (on the basis of theoretical[39] and experimental[2,40,41] evidence) that memory of the incident charge state is lost near the surface. By using the theory of Marston *et al.*, we developed the above detailed picture of the dynamics of resonant charge transfer in alkali ion-metal surface systems which is consistent with a large number of known observations.

Finally, we note that the measured $Li^0(2p)$ yield for $E_i = 100$ eV (see Fig. 4) shows a small increase at the lowest work functions. This feature is not reproduced by the present implementation of the theory of Onufriev and Marston.[42] At present, we do not have an explanation for this increase. However, we can say that it is highly unlikely that the scattering cross section increases rapidly enough to account for the observed increase in the signal. Also, autoionization processes, which might produce ions during the hard collision with the surface, followed by the neutralization of these ions into the $Li^0(2p)$ state on the outgoing trajectory, are less likely for collisions with $E_i = 100$ eV than for collisions with $E_i = 400$ eV.[37]

VI. SUMMARY

In this paper, we presented measurements of the relative probability of $Li^0(2p)$ formation as a function of the adsorbate-induced work-function change when hyperthermal energy Li^+ ions are incident on K/Cu(001) and Cs/Cu(001), along the $\langle 100 \rangle$ azimuth. The probability is broadly peaked with decreasing work function. A theoretical model which solves the time-dependent Anderson-Newns Hamiltonian and allows for the formation of positive ions, electron-hole pairs, neutral ground-state atoms, neutral excited-state atoms, and negative ions has been used to interpret the data. The model suggests that the origins of the peak in the excited-state yield are the decreasing difference between the energy of the $Li^0(2p)$ state and the Fermi level, and the competition between the excited state and the negative ion state. Also, differences between the $Li^0(2s)$ and $Li^0(2p)$ lifetimes play a role in the peak formation as does electron-hole pair formation.

ACKNOWLEDGMENTS

We thank Eric Dahl, David Goodstein, and Craig Keller for many useful discussions. We also thank Peter Nordlander, Jean-Pierre Gauyacq, and Dominique Teillet-Billy for giving us the results of their lifetime calculations for use in this study. This research was funded by the Air Force Office of Scientific Research (AFOSR-91-0137), by the National Science Foundation (NSF-DMR-9022961), and the Cornell Materials Science Center (NSF-DMR-9121654). D.R.A. was also supported by the Swedish Institute and the Sweden-America Foundation. J.B.M. was partially supported by the National Science Foundation (NSF-DMR-9357613).

*Present address: The Department of Physics and Astronomy, 303 Strong Hall, Eastern Michigan University, Ypsilanti, MI 48197.

†Present address: Department of Applied Physics, Chalmers University of Technology, S-41296 Göteborg, Sweden.

[1] E. R. Behringer, D. R. Andersson, B. H. Cooper, and J. B. Marston, preceding paper, Phys. Rev. B **54**, 14 765 (1996).

[2] J. Hermann, B. Welle, J. Gehring, H. Schall, and V. Kempter, Surf. Sci. **138**, 570 (1984).

[3] J. Hermann, J. Gehring, and V. Kempter, Surf. Sci. **171**, 377 (1986).

[4] H. Schall, W. Huber, H. Hoermann, W. Maus-Friedrichs, and V. Kempter, Surf. Sci. **210**, 163 (1989).

[5] H. Schall, H. Brenten, K. H. Knorr, and V. Kempter, Z. Phys. D **16**, 161 (1990).

[6] H. Brenten, K.-H. Knorr, D. Kruse, H. Müller, and V. Kempter, Nucl. Instrum. Methods Phys. Res. Sect. B **48**, 344 (1990).

[7] E. R. Behringer, D. R. Andersson, D. M. Goodstein, B. Kasemo, B. H. Cooper, and J.B. Marston, Nucl. Instrum. Methods Phys. Res. Sect. B **78**, 3 (1993).

[8] D. R. Andersson, E. R. Behringer, B. H. Cooper, and J. B. Marston, J. Vac. Sci. Technol. A **10**, 2196 (1993).

[9] J. B. Marston, D. R. Andersson, E. R. Behringer, C. A. DiRubio, G. A. Kimmel, C. Richardson, and B. H. Cooper, Phys. Rev. B **48**, 7809 (1993).

[10] R. L. McEachern, D. L. Adler, D. M. Goodstein, G. A. Kimmel, B. R. Litt, D. R. Peale, and B. H. Cooper, Rev. Sci. Instrum. **59**, 2560 (1988).

[11] P. W. van Amersfoort, J. J. C. Geerlings, L. F. Tz. Kwakman, E. H. A. Granneman, and J. Los, J. Appl. Phys. **58**, 2312 (1985).

[12] G. A. Kimmel and B. H. Cooper, Rev. Sci. Instrum. **64**, 672 (1993).

[13] D. M. Goodstein, Ph.D. Thesis, Cornell University, 1990.

[14] SAES Getters/USA Inc., Colorado Springs, CO.

[15] T. Aruga, H. Tochihara, and Y. Murata, Phys. Rev. Lett. **52**, 1794 (1984).

[16] T. Aruga, H. Tochihara, and Y. Murata, Surf. Sci. **158**, 490 (1985).

[17] T. Aruga, H. Tochihara, and Y. Murata, Surf. Sci. **175**, L725 (1986).

[18] J. Cousty, R. Riwan, and P. Soukiassian, Surf. Sci. **152/153**, 297 (1985).

[19] C. A. Papageorgopoulos, Phys. Rev. B **25**, 3740 (1982).

[20] Hammamatsu model R943-02.

[21] D. R. Andersson (private communication).

[22] D. L. Adler and B. H. Cooper, Rev. Sci. Instrum. **59**, 137 (1988).

[23] We used the manufacturer-specified transmissions of the optical elements in the detector (e.g., sapphire window, lenses, fiber optic, and interference filter), the solid angle of acceptance of the input lens, and assumed that the excited atoms radiate isotropically and that the copper sample is perfectly reflecting at 685 nm.

[24] D. M. Newns, Phys. Rev. **178**, 1123 (1969).

[25] P. Nordlander and J. C. Tully, Phys. Rev. B **42**, 5564 (1990).

[26] E. R. Behringer, J. G. McLean, and B. H. Cooper, Phys. Rev. B **53**, 7510 (1996).

[27] E. R. Behringer, Ph.D. thesis, Cornell University, 1994.

[28] J. J. C. Geerlings, L. F. Tz. Kwakman, and J. Los, Surf. Sci. **172**, 257 (1987).

[29] J. J. C. Geerlings, R. Rodink, J. Los, and J. P. Gauyacq, Surf. Sci. **181**, L177 (1987).

[30] G. A. Kimmel, D. M. Goodstein, and B. H. Cooper, J. Vac. Sci. Technol. A **7**, 2186 (1989).

[31] G. A. Kimmel, D. M. Goodstein, Z. H. Levine, and B. H. Cooper, Phys. Rev. B **43**, 9403 (1991).

[32] Z. L. Miskovic, S. G. Davison, and F. O. Goodman, Phys. Rev. Lett. **71**, 4075 (1993).

[33] C. B. Weare and J. A. Yarmoff, J. Vac. Sci. Technol. A **13**, 1421 (1995).

[34] C. B. Weare, K. A. H. German, and J. A. Yarmoff, Phys. Rev. B **52**, 2066 (1995).

[35] C. B. Weare and J. A. Yarmoff, Surf. Sci. **348**, 359 (1996).

[36] K. W. Sulston, A. T. Amos, and S. G. Davison, Surf. Sci. **224**, 543 (1989).

[37] H. Brenten, H. Müller, K. H. Knorr, D. Kruse, H. Schall, and V. Kempter, Surf. Sci. **243**, 309 (1991).

[38] H. Brenten, H. Müller, D. Kruse, and V. Kempter, Nucl. Instrum. Methods Phys. Res. Sect. B **58**, 328 (1991).

[39] R. Brako and D. M. Newns, Surf. Sci. **108**, 253 (1981).

[40] B. Hird, P. Gauthier, J. Bulicz, and R.A. Armstrong, Phys. Rev. Lett. **67**, 3575 (1991).

[41] G. A. Kimmel, Ph.D. thesis, Cornell University, 1992.

[42] Onufriev and Marston recently extended the theory to incorporate the Auger mechanism, and obtained results consistent with the observed increase in the relative yield at low work functions. See A. Onufriev and J. B. Marston, Phys. Rev. B **53**, 13 340 (1996).